

Rod-shaped nanostructures based on superparamagnetic nanocrystals as viscosity sensors in liquid

Marco Allione,^{1,a)} Bruno Torre,¹ Alberto Casu,¹ Andrea Falqui,¹ Philomena Piacenza,² Riccardo Di Corato,^{1,2} Teresa Pellegrino,^{1,2} and Alberto Diaspro¹

¹*Italian Institute of Technology, via Morego 30, I-16163, Genova, Italy*

²*Nanoscience Institute of CNR, National Nanotechnology Laboratory, Via Arnesano 16, 73100 Lecce, Italy*

(Received 11 April 2011; accepted 10 August 2011; published online 21 September 2011)

Superparamagnetic nanostructures are becoming increasingly important as tools for biological and medical applications. We report the study of the movement of rod-shaped assemblies of superparamagnetic nanocrystals under the action of a rotating magnetic field. The dynamic was characterized by means of light scattering detection at different frequencies and for different values of the intensity of the applied external field. The possibility to correlate the motion to the viscosity of the medium is used to monitor viscosity changes inside the liquid. We propose this technique as a valuable tool to monitor viscosity at microscale for application in biological studies. © 2011 American Institute of Physics. [doi:10.1063/1.3638695]

INTRODUCTION

Nanostructures realized with magnetic materials have always drawn a lot of interest for their peculiar properties. Ferromagnetic materials, in particular, once reduced in size down to a single magnetic domain, show the well known phenomenon of superparamagnetism.¹ Furthermore, the recent advances in the field of chemical synthesis of these materials led to the demonstration of the possibility to prepare nanostructured magnetic systems of different shapes that have been proposed for many different kinds of application like, e.g., treatment of tumors,^{2,3} targeted drug delivery⁴ and biosensing.^{5,6}

The fact that they can respond to the action of an external field has been used to transfer energy to them, as in the case of magnetic nanostructures-mediated thermal treatment of tumors, or to accumulate them in particular areas of a biological sample, but it can also be used as a system to monitor frictions inside a sample and sense viscosity in a liquid environment.

A lot of research has been done in recent years to study the self-aggregation of superparamagnetic nanoparticles to form super-structures or higher order aggregates.^{5,7–11} These kinds of systems actually require usually some time to self-assemble under the action of an external field and their length and stability upon motion depend on field strength.⁸ In some of these works, researchers used magnetic field to obtain self-assembly of chains of superparamagnetic nanocrystals and studied them upon rotation or other types of regular periodic motion.^{5,7} More recently, the formation of structures obtained by self-aggregation of superparamagnetic nanocrystals was proposed, that were stabilized by the addition of an external polymeric layer, and their movement upon different types of variable magnetic fields was microscopically analyzed by means of image analysis techniques.^{12–14} Actually, the combination of the preparation

of such kind of structures with the detection of scattered light, already used to test the stability of magnetic field induced self-assembled structures,⁵ can represent a cheap and easy-to-implement detection tool to probe the properties of fluids at microscale.

In this work, we demonstrate that needle-shaped nanostructures can be effectively used as sensors for measuring the viscosity in a liquid medium, by combining the action of an external rotating magnetic field with a very simple optical measurement. In order to do so, we have prepared rigid chains of magnetic nanocrystals enveloped within a polymer shell. These structures are in the micrometer scale range in length and few tens of nanometers in thickness. In this case, the shape is preserved even in absence of an external field thanks to the presence of the polymer coating layer as also shown in other recent publications.^{12,13} Their anisotropic shape is the key to control their orientation by means of an external magnetic field; hence, the coupling of this effect with the use of a non-invasive optical technique allows to monitor their response to the field and to use it as an on-line direct monitor of the surrounding liquid environment viscosity.

SAMPLE PREPARATION AND CHARACTERIZATION

The preparation method is based on the modification of a procedure previously published by some of us for obtaining spherical magnetic polymer beads.^{15,16} The samples were obtained by co-precipitation of iron oxide nanoparticles or alternatively iron manganese oxide nanocrystals and of a polymer, named poly(maleic anhydride *alt*-1 tetradecene), mediated by solvent destabilization in presence of a static magnetic field. Starting with a tetrahydrofuran solution of well dissolved nanocrystals and polymer, the addition of acetonitrile induces a change in the solubility of both the nanocrystals and the polymer and promotes their aggregation. More in details, 10 μ l of chloroform solution of γ -Fe₃O₄ nanocrystals of 9 nm in diameter prepared by thermal

^{a)}Author to whom correspondence should be addressed. Electronic mail: marco.allione@iit.it.

decomposition method, at a concentration of $4.4\ \mu\text{M}$, are first transferred in a 4 ml-vial and dried under a nitrogen flow.

Then $188\ \mu\text{L}$ of tetrahydrofuran (THF) are added to the vial and additional $12\ \mu\text{L}$ of a polymer-stock solution (50mM in THF, concentration measured as monomer polymer units) are added and the solution is shaken for 20 min on a “shaking plate” (900–1000 rpm). A permanent magnet is then placed beneath the vial, which generates a static field of 0.3 T at the sample position, and, under shaking, $800\ \mu\text{L}$ of acetonitrile are added to the mixture at a flow rate of $250\ \mu\text{L}/\text{min}$ (a syringe pump is used for the addition). The procedure can be also extended to MnFe_2O_4 -Nanocrystals (in case of MnFe_2O_4 , the following amount were employed: $10\ \mu\text{L}$ of MnFe_2O_4 nanoparticles $10\ \text{nm}$ in diameter at a concentration of $5.36\ \mu\text{M}$ in chloroform, $10\ \mu\text{L}$ of polymer-solution $50\ \text{mM}$ in THF and an analogous procedure as the one reported for the iron oxide nanoparticles is used for the stick formation). TEM images of the nanocrystals used as building-blocks and an example of the resulting assemblies for both Fe_3O_4 and of MnFe_2O_4 are shown in Figure 1.

Magnetization measurements were performed in a Quantum Design MPMS7XL SQUID magnetometer over a thermal range between 5 and 350 K and applying magnetic fields up to 70 kOe. In particular, zero-field-cooled (ZFC) magnetizations were measured, after cooling the samples in a zero magnetic field, increasing the temperature in a static field of 50 Oe, whereas field-cooled (FC) curves were measured by cooling once again the samples while keeping the same static field. Isothermal magnetizations were measured by varying the applied magnetic field from zero to 70 kOe and again to zero, while keeping the samples in superparamagnetic condition by choosing an adequate temperature (in the present case 298 K). Due to the fact that the mass of magnetic phase could not be precisely measured for the samples here studied, all the results are expressed in terms of absolute longitudinal moment.

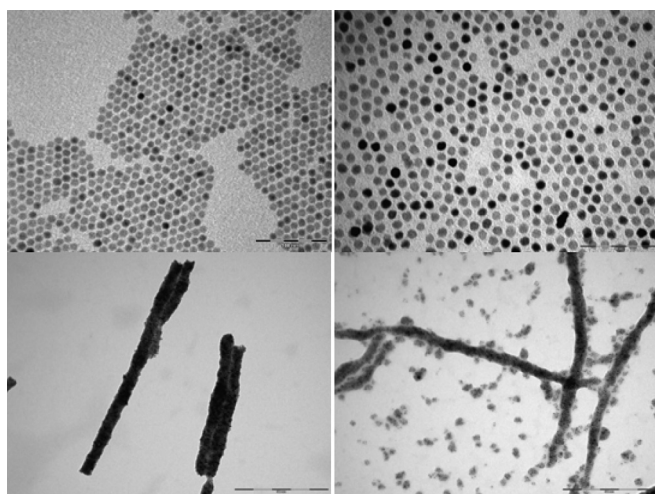


FIG. 1. TEM characterization of the initial nanocrystals and of the corresponding rod-shaped nanostructures obtained. On the upper panels TEM images of the single nanocrystals of Fe_3O_4 (left) and of MnFe_2O_4 (right) are reported. The TEM images of the corresponding aggregated structures are shown in the bottom panels for iron oxide (left) and manganese-iron oxide (right). The scale bars correspond to 100 nm for the two upper panels and 500 nm for the two lower ones.

Solution of nanomagnets, prepared according to the above procedure, have been optically characterized by light scattering experiments: a cuvette of solution containing the nanomagnets in their native solvent was inserted into the center of a four-magnets system, disposed in a crossed dipoles configuration. Four commercial electromagnets were attached to four opposite sides of an aluminum made octagonal support. Each couple of opposite electromagnets was connected in parallel to the output channel of a two-channel home-made power amplifier, driven by a commercial computer-controlled analog output card (National Instruments, model NI USB-6251). The spacing between the magnets was reduced to the minimum possible value in order to leave a small (about 1 mm) aperture to allow the scattered light to reach the detector, in order to keep at maximum the field strength and uniformity in the center of the four-fold symmetric system. Magnetic field in the center of the system was measured by means of a magnetometer in static configuration (i.e., when the current in the two couples of coils was kept constant). It turned out to be well planar and homogeneous around the center of the system with values that depend linearly on the driving voltage in the range 1–10 mT. Scattering measurements were performed by sending a laser beam through the sample from a direction perpendicular to the magnetic quadrupole plane and in the center of symmetry of the octagonal system and collecting the scattered light at 90° from the direction of incidence by means of a commercial silicon-based photodiode. The voltage output was measured by the same computer-controlled analog-to-digital card controlling the magnets driving circuitry. The two signals, driving sinusoidal input and photodiode voltage output, were systematically analyzed by means of software realized in the open-source Scilab (<http://www.scilab.org/>) environment. A schematic diagram of the experimental setup is shown in the upper panel of Figure 2. Since some of the samples, nominally those showing the longest wires, showed the tendency to partially precipitate over a time-scale of several hours, all solutions were shaken in a chemical shaker just before measurement, and each measurement was lasting not more than half an hour.

RESULTS AND DISCUSSION

When an object with a strongly anisotropic shape as the self-assembled rods described here is irradiated with a laser beam, the light scattered by each structure will present strong anisotropy in its angular distribution. In the case of particles randomly oriented in the sample, all contribution will mediate to give a final isotropic light distribution. On the contrary, if an external force is applied to orient the structures, as the external magnetic field does in the present case, all contributions to the scattering coming from each single structure will result in a globally anisotropic angular distribution. A clear example of this in the case of our samples is shown in Figure 2.

The lower panel shows a plot of the intensity of the light scattered by a sample of superparamagnetic nanobars of manganese-iron oxide as a function of the angle of orientation of the magnetic field. Each measurement was taken after

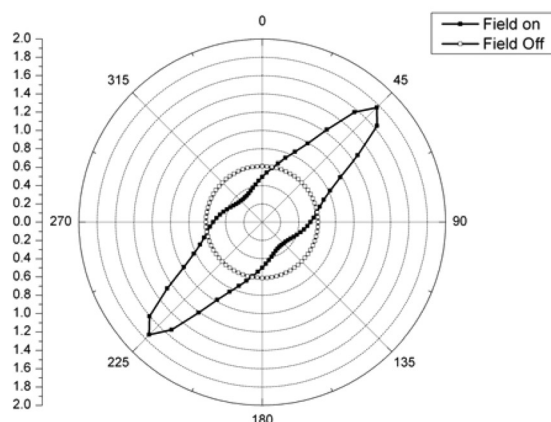
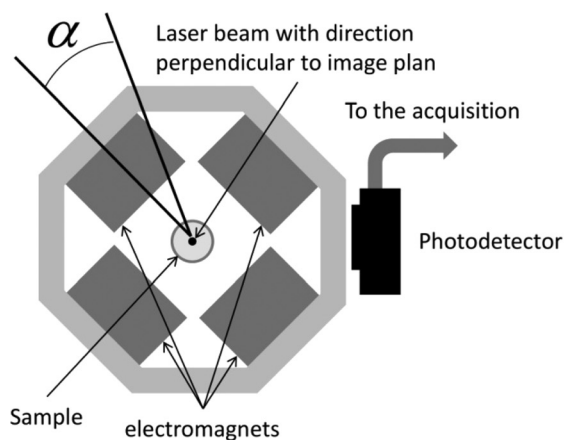


FIG. 2. (upper panel) Schematic diagram of the experimental setup. The angle α represents the angle of orientation of the magnetic field in the experimental frame. (lower panel) Polar plot of the intensity of the light scattered by a sample of nanobars of manganese-iron oxide as a function of the angle of orientation of the magnetic field. The empty symbols represent the intensity of the light scattered by the sample in absence of magnetic field, while the black ones represent the intensity of the scattered light as a function of the angle α . It is clear that the maximum occurs when the rods are oriented toward a direction perpendicular to the direction of the optical detector.

5 s delay in each point before measuring the scattering, in order to be sure that the bars were completely oriented toward the direction of the field. The maximum scattering efficiency takes place in the direction perpendicular to the direction of the field orientation, i.e., of the bars into the liquid solution. The signal is, as expected, symmetrical upon reflection around a plane perpendicular to the bar orientation axis, due to the morphological symmetry of the nanostructures themselves. Experiments performed with nanostructures obtained from different preparations, confirm as expected, that signal anisotropy depends on the average aspect ratio of the nanomagnets population: the higher the aspect ratio, the bigger is the signal anisotropy.

When the structures are submitted to the action of a magnetic field that rotates at a constant angular speed, they will rotate at the same frequency of the external field but its direction will be different from the one of the field. The angle θ between the field and the rod will result from the balance between the applied magnetic torque and an opposite torque due to the presence of a viscous friction between the particle and the surrounding liquid. Obviously, θ depends on

the angular frequency f at which the field is rotating and on the viscosity of the medium η . Similar considerations have already been done in literature for different assemblies of superparamagnetic nanocrystals subject to a field in dynamic or transient movement, either in solution or encapsulated in polymer matrices.^{7,17–19}

The balancing of the magnetic torque induced by dipole-dipole interaction between nanocrystals in the bar and the viscous torque induced on the same bar by its rotation, in the hypothesis of Newtonian, non speed-dependent viscous interaction between the bar and the surrounding liquid, gives the relation for θ :

$$\theta = 1/2 \arcsin(a \eta f / m^2) \quad (1)$$

where a is a factor incorporating the dependence on the geometry of the nanostructure and m is the magnetic dipole moment of each nanocrystal (supposed identical for all of them).

The $1/2$ factor in the equation comes for the symmetry of the system upon reflection from a plane perpendicular to the longitudinal axis of the bars. Apart from the above-mentioned approximation, the result of Eq. (1) relies also on the hypothesis that the inter-particle interaction does not destroy the superparamagnetic character of the system by introducing a global permanent magnetization of the rod.

In order to demonstrate this, we performed magnetic characterization of the samples in two steps. First, their magnetic response was collected in a fixed low magnetic field condition as a function of temperature (ZFC-FC measurements), then it was measured in a fixed temperature condition as a function of applied magnetic field (isothermal magnetization).

The observation of the ZFC and FC curves as a function of temperature pinpoints two different zones, a high-temperature one where a superposition of ZFC and FC curves is found (superparamagnetic state) and a low-temperature one where each curve shows a different magnetic response, with the temperature value T_{SEP} marking the lowest temperature where superparamagnetic behavior is found.²⁰ T_{MAX} is related in a complex way to the mean nanoparticle size of the sample studied and the thermal range below it is referred to as blocked state for the sample.

The tests were performed on two samples, one of the magnetic nanobars used in the optical characterization described above, and the other on the single MnFe_2O_4 nanocrystals not aggregated.

In the present case, the samples showed similar T_{MAX} values, namely $T_{\text{MAX}} = 46$ K for the nanobars sample and $T_{\text{MAX}} = 40$ K for the isolated nanocrystals sample, pointing out that the aggregated bars retain the superparamagnetic behavior of the isolated crystals at room temperature. Most likely, the observed small increase of the T_{MAX} can be ascribed to the presence of inter-particle magnetic interaction among the single nanocrystals in the nanobars.^{21,22}

The measurement of the isothermal magnetization (M vs H curve) at a temperature higher than T_{SEP} was used to confirm their superparamagnetic state, as in that case hysteretic behavior cannot be found: the absence of remanence and

coercivity confirms that at 298 K the aggregated nanobars preserve the superparamagnetic behavior, thus confirming the hypothesis of our model and in agreement with recent results from literature.¹⁴ The ZFC-FC curves of the single nanocrystals sample and of the aggregated nanobars one, with their respective isothermal magnetization curves at 298 K as insets, are shown in Figure 3, upper and lower panel, respectively.

Provided that θ is small enough, Eq. (1) can be simply approximated with

$$\theta = \frac{1}{2} a \eta f / m^2 \quad (2)$$

In our experiment the sample was submitted to the action of an external magnetic field rotating in the plane of two coupled magnetic dipoles. Both signals from the reference driving curve of the magnetic field and of the scattered light collected by our detector were recorded simultaneously, with the second one showing a clear periodical oscillation correlated to the driving magnetic field rotation, but with a frequency which is twice the frequency of the reference input, due to the same axial symmetry that is responsible for the $1/2$ factor in Eq. (1) as discussed above. An example of this behavior of the scattering signal with respect to the driving current signal is reported in the inset in Figure 4 (lower panel).

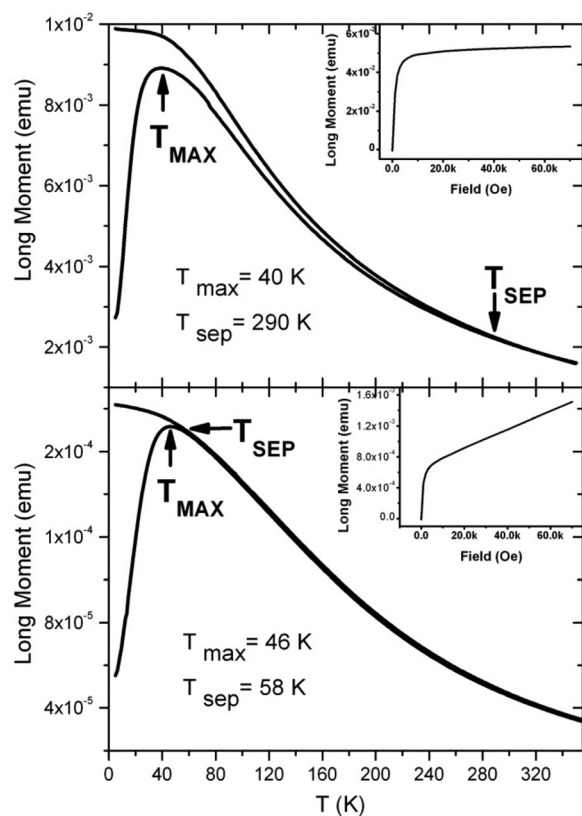


FIG. 3. (upper panel) ZFC-FC curves for a sample of isolated MnFe_2O_4 nanocrystals. To further demonstrate the superparamagnetic behavior of the sample, an isothermal curve taken at 298 K on the same sample is shown in the inset. Results are expressed as absolute value of the longitudinal moment, i.e. the magnetization moment along the axis of the applied field (lower panel). The same as for the upper figure, but for the aggregated magnetic nanobars: the persistence of the superparamagnetic behavior in this sample at room temperature is clearly demonstrated by these curves.

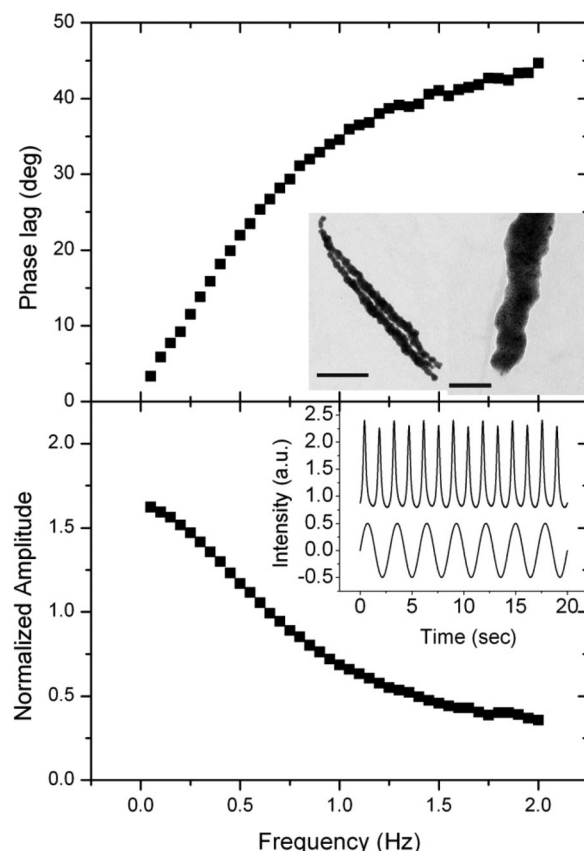


FIG. 4. (upper panel) Phase delay between the sinusoidal current signal that drives the rotation of the magnetic field in the setup and the scattering intensity from the sample collected by the detector. Values, converted in degrees and shifted to give a zero value for the static case (i.e., frequency=0) are plotted as a function of the driving frequency. TEM images refer to the sample used, which is composed by structures made of MnFe_2O_4 nanocrystals. Scale bars are 500 nm for the picture on the left and 100 nm for the one on the right. (lower panel) Normalized modulation amplitude of the scattering signal as a function of the field rotation frequency, calculated as peak-to-valley modulation amplitude divided by the signal mean value. The inset reports an example of the scattering signal evolution in time (upper curve) with its corresponding sinusoidal driving signal, as collected during the experiment.

Figure 4, upper panel, reports the behavior of phase lag θ as a function of the rotation frequency for a solution of nanomagnets obtained from the analysis of the scattering signal. Such values are obtained by extracting from the two curves the relative phase delay between the two signals. It can be seen in this picture that the behavior of the curve deviates from the linear one at higher frequencies, a deviation that cannot be explained even by the more complete Eq. (1). The reason for this is the size dispersion of the sample: each solution contains bars of different lengths (between 1 and 10 μm). At fixed bar length the magnetic torque depends linearly on the length, while the viscous torque exhibits a quadratic dependence on the same parameter assuming a nearest neighbor approximation for the interaction between each single nanocrystal. Therefore a spreading in the angular response of a polydispersed sample is expected since, when increasing angular velocity, at a certain point the longer sticks will no longer be able to follow the rotation due to the excessive viscosity. It is then obvious that this critical cut-off frequency at which the magnet is no more able to

follow the rotation of the magnetic field will depend on the bar length: the longer the bar the lower will be the cut-off frequency. The normalized modulation amplitude of the scattering signal (i.e., the amplitude of the periodic modulation of the signal divided by the signal average value) reported in Figure 3 confirms this: the decrease in the modulation amplitude is a clear indication of the fact that many wires can no longer follow the field rotation and so do not contribute anymore to the scattering modulation. Hence, the evident length dependence of the phase lag of the nanorods with respect to the rotating field, already discussed above, affects the efficiency of the scattered light at the higher frequencies, due to the evident relatively big length dispersion of the sample. Nevertheless, the collection of the scattering phase lag at the lower frequencies, even if it comes from the results over an average on the different lengths in the sample, is able to provide information on the viscosity of the liquid environment.

In order to demonstrate this, a glucose solution in water was used since its viscous properties are well known in literature.²³ In particular for the solution of glucose in pure water the linearity of the dependence of the viscosity coefficient η on the glucose concentration C (in moles per liter) was demonstrated in ref 23. In this work, the viscosity coefficient of the solutions is demonstrated to fit the relation $\eta = \eta_0(1 + BC)$, resulting in a value of 1.12 for the B coefficient at 25 °C. In Figure 5 (upper panel), the frequency scan on three different samples is shown. The samples were prepared by mixing 100 μ l of mother solution of nanomagnets in acetonitrile (AcN) and 400 μ l of purified water (Milli-Q) in three different vials, to which a different quantity of glucose was added. No precipitated glucose was observed in any of the samples after mixture. All of them were measured also many days after preparation giving always comparable results.

The slopes of the obtained curves are reported in Figure 4 (lower panel) as a function of the glucose concentration in the solution. To fulfill the requirement for “small angles” of Eq. (2) only θ values below 1/10 of the semi-rotation (i.e., smaller than 18°) were considered for the calculation of the slopes.

The measurement was repeated with the same nanorods re-dispersed in water after complete AcN evaporation and the slopes obtained in four of such prepared samples are shown in Figure 6.

From the linear fits to the two plots the value of the coefficient B can be derived and it turns out to be (0.63 ± 0.005) in the first case and (1.6 ± 0.1) in the second. The lower value of the coefficient for the mixed solvents solution is compatible with the lower viscosity of AcN with respect to water.²⁴ The coefficient for water turns out to be higher than the one reported in literature, but this could be due to the different scale at which the viscosity is probed in our case and to the particular interaction between the liquid and the nanostructures. A contribution in this sense might also come from the inter-rods interaction. In the described experiment, the rods concentration was kept at minimum in order to minimize this effect, but within the limits imposed by the necessity of detecting a good scattering signal. Friction of one rod with the others around, or simply the interaction between the

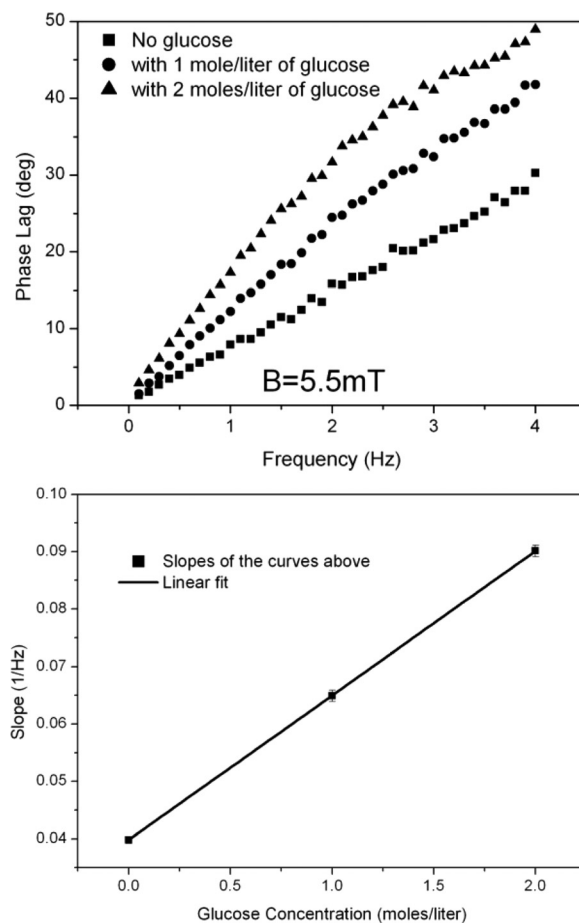


FIG. 5. (upper panel) Phase lag as a function of rotation frequency for three different samples with different glucose concentration in a solution of mixed water and AcN (80 and 20%vol., respectively). (lower panel) Slope of the three curves in the upper panel for small values of the phase delay as a function of the glucose concentration in the solution. The starting solution of nanomagnets was the same as used for Figure 3.

small vortex generated by liquid rotation around each rod, can in fact introduce an extra contribution to friction that might partially explain the over-estimate of the viscosity coefficient.

The precision with which it is possible to determine the viscosity change is actually represented by the error bars in

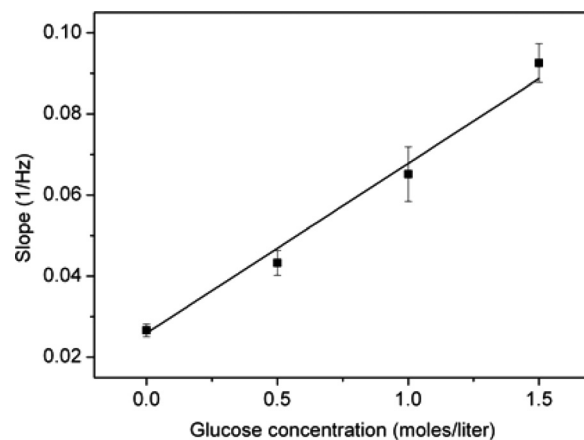


FIG. 6. Measurement on the same nanomagnets used for measures reported in Figure 4 re-dispersed in water after complete AcN drying.

the graph. In the case of Figure 5, a relative standard deviation on the value of viscosity in the order of 1.5% can be deduced by the linear fits. This uncertainty in the determination of the viscosity is actually comparable or slightly higher than the one obtained with more conventional methods, but the interests in this technique lays rather on the possibility to probe in principle also very small quantity of liquid and without having to manipulate or remove it from its original environment, a thing that can be of relevant interests in many applications, notably in biophysics. The higher error bars and the larger scattering of the data points in Figure 6 are attributed to the presence of aggregates and a stronger trend of the sample to precipitate shown by the samples prepared in this way. This is attributed to the formation of big irregular aggregates in the solution that were a consequence of this preparation and that were actually observed under an optical microscope and this is the reason why the uncertainty on the B coefficient value turns out to be noticeably higher in this case. This hints to the importance of high quality solutions for the determination of the viscosity with higher accuracy since big aggregates contribute strongly to the scattered signal from the sample.

CONCLUSIONS

In conclusion, we have demonstrated that it is possible to monitor the viscosity of a liquid solution by means of needle-shaped nanocomposite made of superparamagnetic nanocrystals, by using a very simple optical technique. This tool is potentially able to follow even quite small viscosity changes in the solution with a measurement that, if automated, can be performed within few minutes with a very cheap and easy-to-realize optical setup. Moreover, our measurements do not require nanostructure self-assembly as in other similar tests reported in literature,^{7,19} since the anisotropic shape of our structures is preserved by its polymer capping. These tests prove in any case that these nanomagnets can be a valuable tool to probe viscosity in a liquid solution and can monitor its changes, potentially also at the micrometer length scale. The system in fact can in principle be used to get rheological information at the micrometer scale by analyzing the motion of single nanomagnets. Investigations in this direction are currently performed in our lab.

ACKNOWLEDGMENTS

We thank Alberto Barone, Luca Ceseracciu and Riccardo Carzino for a critical revision of the manuscript and for fruitful discussions. This work was partially supported by the European project Magnifyco (Contract NMP4-SL-2009-228622).

- ¹G. C. Papaefthymiou, *Nano Today* **4**, 438 (2009).
- ²D.-H. Kim, E. A. Rozhkova, I. V. Ulasov, S. D. Bader, T. Rajh, M. S. Lesniak, and V. Novosad, *Nature Mater.* **9**, 165 (2010).
- ³F. Gazeau, M. Levy, and C. Wilhelm, *Nanomedicine* **3**, 831 (2008).
- ⁴M. Arruebo, R. Fernández-Pacheco, M. R. Ibarra, and J. Santamaría, *Nanotoday* **2**, 22 (2007).
- ⁵S. Y. Park, H. Handa, and A. Sandhu, *Nano Lett.* **10**, 446 (2010).
- ⁶A. Figuerola, R. Di Corato, L. Manna, and T. Pellegrino, *Pharmacol. Res.* **62**, 126 (2010).
- ⁷C. Wilhelm, J. Browaeys, A. Ponton, and J.-C. Bacri, *Phys. Rev. E* **67**, 011504 (2003).
- ⁸G. Bertoni, B. Torre, A. Falqui, D. Fragouli, A. Athanassiou, and R. Cingolani, *J. Phys. Chem. C* **115**, 7249 (2011).
- ⁹M. Varón, L. Peña, L. Balcells, V. Skumryev, B. Martinez, and V. Puentes, *Langmuir* **26**, 109 (2010).
- ¹⁰D. Fragouli, R. Buonsanti, G. Bertoni, C. Sangregorio, C. Innocenti, A. Falqui, D. Gatteschi, P. D. Cozzoli, A. Athanassiou, and R. Cingolani, *ACS Nano* **4**, 1873 (2010).
- ¹¹Despina Fragouli, Bruno Torre, Giovanni Bertoni, Raffaella Buonsanti, Roberto Cingolani, and Athanassia Athanassiou, *Microsc. Res. Techniq.* **73**, 952 (2010).
- ¹²J. Fresnais, J.-F. Berret, B. Frka-Petesic, O. Sandre, and R. Perzynski, *Adv. Mater.* **20**, 3877 (2008).
- ¹³J. Fresnais, J.-F. Berret, B. Frka-Petesic, O. Sandre, and R. Perzynski, *J. Phys.: Condens. Matter* **20**, 494216 (2008).
- ¹⁴B. Frka-Petesic, K. Erglis, J. F. Berret, A. Cebers, V. Dupuis, J. Fresnais, O. Sandre, and R. Perzynski, *J. Magn. Magn. Mater.* **323**, 1309 (2011).
- ¹⁵R. Di Corato, N. Bigall, A. Ragusa, D. Dorf, A. Genovese, R. Marotta, L. Manna, and T. Pellegrino, *ACS Nano* **5**, 1109 (2011).
- ¹⁶R. Di Corato, P. Piacenza, M. Musarò, R. Buonsanti, P. D. Cozzoli, M. Zambianchi, G. Barbarella, R. Cingolani, L. Manna, and T. Pellegrino, *Macromol. Biosci.* **9**, 952 (2009).
- ¹⁷S. Melle, G. G. Fuller, and M. A. Rubio, *Phys. Rev. E* **61**, 4111 (2000).
- ¹⁸D. Fragouli, R. Buonsanti, G. Bertoni, C. Sangregorio, C. Innocenti, A. Falqui, D. Gatteschi, P. D. Cozzoli, A. Athanassiou, and R. Cingolani, *ACS Nano* **4**, 1873 (2010).
- ¹⁹C. Wilhelm, *Phys. Rev. Lett.* **101**, 028101 (2008).
- ²⁰L. Néel, *Ann. Geophys. (C.N.R.S.)* **5**, 99 (1949).
- ²¹J. L. Dormann, D. Fiorani, and E. Tronc, *J. Magn. Magn. Mater.* **202**, 251 (1999).
- ²²M. El-Hilo, R. W. Chantrell, and K. J. O'Grady, *Appl. Phys.* **84**, 5114 (1998).
- ²³P. S. Nikam, H. R. Ansari, and M. Hasan, *J. Mol. Liq.* **87**, 97 (2000).
- ²⁴Sigma-Aldrich solvents technical datasheets.